Measurement report: Molecular characteristics of cloud water in southern China and insights into aqueous-phase processes from Fourier Transform Ion Cyclotron Resonance Mass Spectrometry

Wei Sun[1,2], Yuzhen Fu[1,2], Guohua Zhang[1,3], Yuxiang Yang[1,2], Feng Jiang[1,2,a], Xiufeng Lian[1,2,b], Bin Jiang[1], Yuhong Liao[1], Xinhui Bi[1,3], Duohong Chen[4], Jianmin Chen[5], Xinming Wang[1,3], Jie Ou[6], Ping'an Peng[1], Guoying Sheng[1]

[1] State Key Laboratory of Organic Geochemistry and Guangdong Key Laboratory of Environmental Protection and Resources Utilization, Guangzhou Institute of Geochemistry, Chinese Academy of Sciences, Guangzhou, 510640, PR China

[2] University of Chinese Academy of Sciences, Beijing, 100049, PR China

[3] Guangdong-Hong Kong-Macao Joint Laboratory for Environmental Pollution and Control, Guangzhou Institute of Geochemistry, Chinese Academy of Sciences, Guangzhou 510640, PR China

[4] State Environmental Protection Key Laboratory of Regional Air Quality Monitoring, Guangdong Environmental Monitoring Center, Guangzhou 510308, PR China

[5] Shanghai Key Laboratory of Atmospheric Particle Pollution and Prevention, Department of Environmental Science and Engineering, Fudan University, Shanghai 200433, PR China

[6] Shaoguan Environmental Monitoring Center, Shaoguan 512026, PR China

[a] now at: Institute of Meteorology and Climate Research, Karlsruhe Institute of Technology, Eggenstein-Leopoldshafen 76344, Germany

[b] now at: Institute of Mass Spectrometry and Atmospheric Environment, Guangdong Provincial Engineering Research Center for On-line Source Apportionment System of Air Pollution, Jinan University, Guangzhou 510632, PR China

Correspondence to: Xinhui Bi (bixh@gig.ac.cn)

Abstract. Characterizing the molecular composition of cloud water could provide unique insight into the aqueous chemistry. Field measurement was conducted at Mt. Tianjing in southern China during May, 2018. Thousands of formulas ($C_{5-30}H_{4-55}O_{1-15}N_{0-2}S_{0-2}$) were identified in cloud water by Fourier transform-ion cyclotron resonance mass spectrometry (FT-ICR MS). CHON represents the dominant component (43.6-65.3% of relative abundance), followed by CHO (13.8-52.1%). S-containing formulas constitute the remaining ~10-20%. Molecules have O/C of 0.45-0.56 and the double-bond equivalent of 5.10-5.70. More than 90% are assigned as aliphatic and olefinic species. No statistical difference of oxidation state is observed between cloud water and interstitial $PM_{2.5}$. CHON with aromatic structures are abundant in cloud water, suggesting their enhanced in-cloud formation. Other organics in cloud water are mainly from biomass burning and oxidation of biogenic volatile organic compounds. The cloud water contains more abundant CHON and CHOS at night, which are mainly contributed by $-N_2O_5$ function and organosulfates, demonstrating the enhanced formation in dark aqueous or multi-phase reactions. While more abundant CHO are observed during the daytime, likely due to the photochemical oxidation and photolysis of N-/S-containing formulas. The results provide an improved understanding on the in-cloud aqueous-phase reactions.

35 **1 Introduction**

36 On average, approximately 70% of the Earth is covered by clouds (Stubenrauch et al., 2013; Herrmann et al., 2015). Cloud

37 water is an important sink of organics (Herckes et al., 2013) and provides a medium for the aqueous-phase reactions of

38 dissolved gases and aerosols (Blando and Turpin, 2000), which can substantially modify the characteristics of the organics

39 (McNeill, 2015; Kim et al., 2019). Aqueous-phase secondary organic aerosols (aqSOA) forming in the in-cloud aqueous-phase

40 processes   significantly contribute to the total SOA with a negative impact for the visibility, human health and climate (Ge et

41 al., 2012; Huang et al., 2018; Schurman et al., 2018; Li et al., 2020a; Smith et al., 2014; Paglione et al., 2020; Hallquist et al.,

42 2009). Therefore, an understanding of the molecular characteristics and aqueous-phase reactions in cloud droplets is crucial to

43 assessing their impact accurately.

44 Organics in cloud water mainly include organic acids (e.g., formic, acetic, oxalic acids and other short-chain mono and

45 dicarboxylic acids) (Sun et al., 2016), carbonyls (e.g., formaldehyde, acetaldehyde, glyoxal and methyglyoxal) (Ervens et al.,

46 2013; Van Pinxteren et al., 2016), as well as some heteroatom-containing compounds such as amino acids (Bianco et al.,

47 2016b), organonitrates, and organosulfates (Zhao et al., 2013). Some less polar organics such as n-alkanes (Herckes et al.,

48 2002), benzene, toluene, ethylbenzene and xylenes (Wang et al., 2020), polycyclic aromatic hydrocarbons (Herckes et al.,

49 2002; Ehrenhauser et al., 2012), phenols and nitrophenols (Lüttke et al., 1997; Lüttke et al., 1999) are also observed, though

50 with a much lower fraction of dissolved organic materials (usually < 1%). The organics that have been characterized using

51 chromatographic and spectroscopic techniques only take a proportion of ~20% of all kinds of organics in cloud water (Herckes

52 et al., 2013; Bianco et al., 2018). Ultra-high resolution mass spectrometry such as Fourier Transform Ion Cyclotron Resonance

53 Mass Spectrometry (FT-ICR MS) has made possible to characterize individual molecular formulas in complex mixtures (Cho

54 et al., 2015). In studies using ultra-high resolution MS to characterize cloud/fog water, formulas were mainly divided into

55 CHO, CHON, CHOS and CHONS based on the elemental composition, in which CHO and CHON were usually dominant

56 (Zhao et al., 2013; Cook et al., 2017; Brege et al., 2018; Bianco et al., 2018; Bianco et al., 2019). Boone et al. (2015) observed

57 a high fraction of N-containing formulas in cloud water compared with particles and attributed it to the aqueous-phase

58 formation. However, a more recent study carried out in Po Valley observed more CHO formulas in cloud water, while particle

59 samples contained more N- and S-containing formulas. The authors attribute it to the high possibility of reactions with sulfate

60 and nitrate ions in the concentrated environment of aerosol liquid water (Brege et al., 2018). Thus more observations are

61 needed to provide more convincing evidences of in-cloud aqueous-phase reactions.

62 Aqueous-phase reactions have been identified as an important source of organics in cloud water in addition to the gas-liquid

63 and particle-liquid partition. Aqueous-phase reactions mainly include radical and non-radical reactions. Under irradiation,

64 hydroxyl radical (OH•) is the main radical in the atmosphere (Herrmann et al., 2010). In cloud water, the oxidation of

65 precursors can be initiated by the hydrogen abstraction or electron transfer reaction driven by the OH•, resulting in the

66   formation of organic acids and condensed compounds (McNeill, 2015). On the one hand, photolysis causes the fragmentation

67   of high-molecular-weight organic compounds, results in the formation of relatively low-molecular-weight compounds such as

68   small acids, including oxalic, glyoxylic and, in large quantity, formic and acetic acid (Renard et al., 2015; Schurman et al.,

69   2018; Huang et al., 2018; Sun et al., 2010; Li et al., 2014; L.Oflund et al., 2002). These compounds are highly oxygenated

70   owing to cloud processing (Brege et al., 2018; Sareen et al., 2016), as indicated by the fact that aqSOA has a higher O/C ratio

71   (~1) than gas-phase SOA (0.3-0.5) in the atmosphere (Ervens et al., 2011). On the other hand, photolysis also lead to the

72   oligomerization of organics, such as pyruvic acid, phenols and methyl vinyl ketone under conditions relevant to deliquesced

73   aerosols (Reed Harris et al., 2014; Renard et al., 2015; Yu et al., 2016). The oligomerization of tryptophan were also observed

74   in synthetic cloud water (Bianco et al., 2016a). For the N- and S-containing organics, photochemistry may also cause the

75   release of inorganic nitrate and sulfate (Braman et al., 2020; Laskin et al., 2015; Bruggemann et al., 2020). The main radicals

76   in the atmosphere at night is $NO_3\bullet$, which can form from the gas-phase reaction between NO_2 and O_3 and enter into cloud

77   droplets. The reactions between $NO_3\bullet$ and organics lead to the oxidation of organics or the addition of functional groups

78   containing N atoms when the aqueous phase is concentrated and acidic (Herrmann et al., 2015; McNeill, 2015; Wang et al.,

79   2008; Szmigielski, 2016; Rudziński and Szmigielski, 2019). Meanwhile, the radical nitration is believed to form

80   dinitroaromatics in the aqueous-phase (Kroflic et al., 2015). Carbonyls can also react with ammonium and amine without

81   illumination, resulting in the generation of imidazoles and N-containing oligomers, especially in aerosol liquid water and

82   evaporating cloud water (De Haan et al., 2009; Kua et al., 2011; De Haan et al., 2011; De Haan et al., 2018). While,

83   organosulfates are formed mainly through heterogeneous and bulk particle phase reactions (Bruggemann et al., 2020). The

84   non-radical reactions in the aqueous phase also include hydrolysis, hydration, acid catalysis, Fenton reaction and translation

85   metals reactivity with organics, probably ozone reactivity at the gas/liquid interface and so on (McNeill, 2015; Deguillaume

86   et al., 2005; Herrmann et al., 2015).

87   To date, only a few studies reported the molecular characteristics of cloud water using ultra-high resolution MS, hampering

88   our understanding of aqueous-phase reactions on the composition of cloud water. In this study, cloud water and $PM_{2.5}$ samples

89   at a remote mountain site were collected and analyzed by FT-ICR MS. The primary objectives of this study are to investigate

90   the molecular characteristics and composition of the organics in cloud water, and to explore the potential influences of aqueous-

91   phase reactions.

92   **2 Materials and methods**

93   **2.1 Sample collection**

94   A sampling campaign was carried out at an atmospheric monitoring station (112°53′56″E, 24°41′56″N, 1690 m above sea

95   level) located in the Tianjing Mountain in southern China (Fig. S1). The site is located in a natural conservation zone far away

96   from anthropogenic activities, which is affected mainly by local biogenic emissions and long-distance transport during the

97   monsoon seasons.

98   A Caltech Active Strand Cloudwater Collector, *Version 2* was used for cloud water collection (Demoz et al., 1996). Sampling

99   methods are presented in Supporting Information (Text S1). A total of 24 cloud water samples (CL1-24) were collected in

100   succession during a long-duration cloud event that lasted from May 8 to May 13, 2018. To investigate the molecular

101   characteristics of the organic compounds and the effects of aqueous-phase processes, six samples collected from May 11 to

102   May 12 (ID: CL12-17, Table 1) were selected for FT-ICR MS analysis in detail since these six samples were all collected

103   during the maintenance stage of a cloud event with stable pH (Table 1), meteorological conditions and no dramatic change of

104   air masses origin (Fig. S1, S2). The sampling interval of six samples are presented in Table 1 and Fig. S2. The samples CL12,

105   CL13 and CL14 were collected during the daytime of May 11, while the other three samples (CL15, CL16 and CL17) could

106   be roughly regarded as nighttime samples although the CL15 was partly collected in the evening.

107   An aerosol sampler (PM-PUF-300, Mingye Inc., China) with a cut size of 2.5 μm was used to collected the interstitial particles

108   ($PM_{2.5}$) at a flow rate of 300 L min^{-1} during the investigated cloud event. The sampling interval of $PM_{2.5}$ was roughly 24 hours.

109   Two $PM_{2.5}$ samples were collected during May 11-13. The details have been provided in Supporting Information (Text S2).

110   **2.2 Sample pretreatment, instrumental analysis, and data processing**

111   Water-soluble organic compounds in cloud water were isolated using solid-phase extraction (SPE) and analyzed using an

112   electrospray ionization (ESI) source coupled with FT-ICR MS in the negative ion mode. $PM_{2.5}$ samples were first ultrasonically

113   extracted with water and then pretreated and analyzed using the same methods with cloud water samples (Text S3). The details

114   of the molecular characteristics of the two $PM_{2.5}$ samples are beyond the scope of this study. However, we documented the

115   main results of the $PM_{2.5}$ samples for the contrastive analysis in the Supporting Information (Fig. S4, S5; Table S3, S4).

116   Kendrick mass defects analysis was used for the formula assignment (Shi et al., 2012). The chemical formula $C_cH_hO_oN_nS_s$

117   with molecular weight of 150-1000 Da was obtained finally. Relative abundance (RA) of each formula was represented by the

118   intensities of each peaks after normalization by the maximum intensity in each sample. Note that ESI FT-ICR MS is not a

119   purely quantitative technique, the intensity of the peak for each formula is a product of its concentration and ionization

120   efficiency. However, since all of the samples were measured using the same instrumental conditions, each spectrum was biased

121   in an equal fashion, so relative peak intensities within the acquired spectra can be compared to each other, although they cannot

122   be related back to concentrations in the original samples (Sleighter et al., 2010; Wozniak et al., 2014).

123   The RA-weighted average elemental ratios of oxygen, carbon, and hydrogen, including O/C_w and H/C_w, the oxidation state of

124   carbon (OS_{Cw}), the double-bond equivalent (DBE_w), and the modified aromaticity index (AI_{mod}) were calculated. OS_C, DBE

125   and AI_{mod} are the parameters, which are generally used to evaluate the average oxidation state of carbon atoms (Kroll et al.,

126   2011), the degree of unsaturation of molecules (Hockaday et al., 2006), and the degree of aromaticity in molecular formulas,

127 respectively (Koch and Dittmar, 2006). The discussion in this paper is based on the weight-average values unless otherwise

128 specified; thus, the subscript "w" is omitted for brevity in the following texts. Details of SPE pretreatment, instrumental

129 analysis and data processing were described in Text S3.

130 In addition, oxalate and water-soluble inorganic ions, and water-soluble organic nitrogen (WSON) in cloud water samples

131 were analyzed using ion chromatograph (IC) and TOC/TN analyser. Details have been provided in Text S3. The 72 h back

132 trajectories were displayed using the Hybrid Single-Particle Lagrangian Integrated Trajectory model

133 (https://ready.arl.noaa.gov) (Stein et al., 2015; Lin et al., 2017). The meteorological conditions during sampling and water-

134 soluble ions concentrations are provided and discussed in Text S4.

135 **3. Results and Discussion**

136 **3.1 Overview of molecular formulas of cloud water and comparison to the interstitial $PM_{2.5}$**

137 A total of 1691, 1546, 1604, 1264, 2364, and 2767 molecular formulas were identified in CL12-17 samples, respectively.

138 According to the elemental compositions, four groups (CHO, CHON, CHOS and CHONS) were assigned. The reconstructed

139 mass spectrum of a typical sample, CL12, is presented in Fig. 1a. The peaks of formulas are intensive within m/z 200-400. A

140 similar pattern is also found in cloud (Zhao et al., 2013; Bianco et al., 2018; Cook et al., 2017), fog (Brege et al., 2018), and

141 aerosols (Lin et al., 2012; Mazzoleni et al., 2012).

142 In cloud water, CHON is the most frequently observed group, representing more than 60% of the total number of assigned

143 formulas. CHO contributes to 16.3-28.3% of the total number of identified formulas, while the proportions of S-containing

144 formulas (CHOS and CHONS) are much lower (3.6-9.4% and 3.7-9.3%, respectively) (Table S5). RA of each group is

145 evaluated, as shown in Fig. 1b and Table S5. The fraction in RA (f_{RA}) of the CHON group is 43.6-65.3% (54.9% on arithmetic

146 average), and CHO contributes 13.8-52.1% (34.7% on arithmetic average). S-containing formulas constitutes the remaining

147 fraction, approximately 10-20% (Table S5). The fraction of four groups in RA and in number are different, which is mainly

148 attributed to some formulas with high intensities contributing much more to RA than to the number.

149 The cloud water shows distinct pattern of molecular composition with the interstitial $PM_{2.5}$. In two $PM_{2.5}$ samples, 1198 and

150 1057 formulas are identified, in which CHO and CHON are dominant. CHO group contributes to 39.9-49.8%, while CHON

151 group contributes to 31.8-51.0%. The S-containing formulas constitutes the remaining fraction of 9.1-18.4%. Similar results

152 can also be obtained by f_{RA} of CHO (44.0-55.5%), CHON (24.3-47.3%) and S-containing formulas (8.7-20.3%) (Table S3).

153 Obviously, the molecular composition of $PM_{2.5}$ in this study is different from that of aerosols in the Pearl River Delta (PRD).

154 More than a half number of all detected formulas were assigned as CHO, while CHON only accounted 8-18% in the aerosols

155 collected at three sites in PRD (Lin et al., 2012). The higher fraction of CHON in cloud water compared with $PM_{2.5}$ at urban

156   and rural areas and interstitial particles is consistent with the pervious finding (Boone et al., 2015), likely indicating the

157   formation of N-containing organics in cloud water.

3.2 Effects of cloud processing on oxidation metrics and aromaticity of the molecular formulas

159   **Oxidation metrics** O/C and OS_C are employed to evaluate the oxidation degree of molecules in cloud water. In six cloud water

160   samples, the average O/C values range from 0.45 to 0.56 (Table S6). No significant differences of O/C are observed between

161   cloud water and $PM_{2.5}$, of which average O/C values are 0.45-0.56. In the Van Krevelen (VK) plot, CHON formulas distribute

162   in a wide area (Fig. 2 and Fig. S6). Some of them with O/C exceeding 0.8 distribute in the top-right corner of the plots, which

163   also result in higher O/C (0.51-0.62, Table S6) of CHON on average compared with CHO, of which O/C ratios range from

164   0.34 to 0.46. On RA-weighted average, the O/C ratios of CHOS and CHONS range from 0.36 to 0.51 and from 0.65 to 0.88,

165   respectively. This is not unintelligible if we note that the N and S atoms in the CHON and S-containing formulas would

166   probably combine with O (e.g., $-NO_2$, $-NO_3$ or $-SO_3$ function group), leading to the higher average O/C of non-CHO formulas.

167   The OS_C value excludes the influence of oxygen atoms combined with H, N, and S, thus it is a more applicative proxy to

168   evaluate the oxidation state of carbon atoms. The average OS_C values range from -0.91 to -0.72 in cloud water (Table S6),

169   while that in $PM_{2.5}$ ranges from -0.84 to -0.61 (Table S4). Being limited by the sampling size, no statistical difference of OS_C

170   can be identified between cloud water and $PM_{2.5}$. However, a higher OS_C of detected formulas, especially CHO, appears in

171    $PM_{2.5}$ samples (-0.40 in P2 sample). Similar phenomenon is also observed in CHOS. It is not consistent with the current

172   understanding that aqueous-phase reactions generally increase the degree of oxidation (Ervens et al., 2011). However, a

173   previous aircraft sampling also observed a lower O/C in cloud water compared with the below-cloud atmospheric particles

174   (Boone et al., 2015), suggesting that the effects of aqueous-phase reaction may be complex in the actual atmosphere. We note

175   that $PM_{2.5}$ samples were collected during the cloud event, high aerosol liquid water content in $PM_{2.5}$ likely provide a sink

176   containing more concentrated precursors for the aqueous-phase reactions compared with cloud water. However, no formation

177   mechanism of more oxidized organics in aerosol liquid water is proposed in previous studies, thus the future researches of

178   aqueous-phase reactions in atmosphere are needed. In four groups, CHO has the highest OS_C values (-0.80 ~ -0.54) (Table S6),

179   which may be related to the high abundance of carboxyl groups in CHO.

180   To investigate the diurnal variation of oxidation metrics in cloud water, daytime and nighttime samples are compared. The

181   O/C ratios show no identified diurnal variation expect for CHO groups. The O/C ratios and OS_C of CHO collected during the

182   daytime is slightly lower than the nighttime (Table S6), this is not consistent with the high oxidation capacity under the

183   illumination during the daytime, indicating that the oxidation degree of the organics in cloud water is not exclusively affected

184   by the illumination.

185   **Aromaticity** The unsaturation and aromaticity of molecular formulas could be evaluated using the H/C ratio and the DBE,

186   where low H/C and high DBE indicate high degree of unsaturation, and to some extent, aromatic structure. On average, H/C

187   ratios in cloud water ranged from 1.44 to 1.49, with no statistic difference compared to $PM_{2.5}$ (1.40-1.53). In the VK plot,

188   CHOS and CHONS occupy an upper area of the diagram with high H/C ratios, indicating that they may have higher saturation

189   compared with CHO and CHON. On average, DBE values in cloud water range from 5.10 to 5.70 (Table S6), which is

190   generally higher than that in $PM_{2.5}$ (4.74-5.04, Table S4). The RA-weighted DBE values of CHO, CHON, CHOS and CHONS

191   are 4.96-6.12, 5.44-6.09, 2.72-4.58 and 3.01-4.29, respectively. DBE values are also projected onto the plots of DBE versus

192   carbon atom number (Fig. 3). DBE values generally increase with carbon number, and CHOS and CHONS distribute in a

193   range with low DBE values. The higher unsaturation degree of CHO and CHON is likely corresponding to the high abundance

194   of aromatic functions.

195   Another commonly used metric of aromaticity is AI_{mod}. In cloud water, most of the formulas (94.9-98.3% of CHO, 79.2-97.5%

196   of CHON, 93.5-98.8% of CHOS and 95.7-100.0% of CHONS in f_{RA}) are assigned as aliphatic or olefinic compounds (Table

197   S7). The f_{RA} of aliphatic and olefinic compounds in $PM_{2.5}$ also exceeds 90%. The high fraction of aliphatic and olefinic and

198   the low fraction of aromatic structure are also observed in aerosol and cloud water in previous studies (Brege et al., 2018; An

199   et al., 2019), however, it is quite different with the primary emissions including biomass burning and coal combustion, of

200   which the fraction of aromatic structures is higher (Song et al., 2018), indicating the aging processes of organics likely reduce

201   the aromaticity of organics. In four groups of molecules in cloud water, CHON has the most (2.5-20.8% in f_{RA}) aromatic

202   structures, consistent with the high DBE values (unsaturation) of CHON. Previous studies conducted in the Po Valley, Italy

203   (Brege et al., 2018) and Fresno, USA (Leclair et al., 2012) also observed the higher fraction of aromatics in CHON compared

204   with the S-containing groups in fog water. The dinitrophenols in cloud water contributes to the high f_{RA} of aromatic structures

205   in CHON significantly, which may be related to the aqueous-phase reactions (see the detailed discussion in Section 3.4).

206   **3.3 Molecular composition of cloud water**

207   **CHON** In cloud water, CHON formulas show no prominent carbon number peaks except sample CL17 (Fig. S7), and one or

208   two nitrogen atoms are assigned to them (Fig. 4). Both the N_1 and N_2 categories contain 1-14 oxygen atoms. The most abundant

209   class of N_1 formulas is $-N_1O_8$ or $-N_1O_7$ (Fig. 4), which include $C_{12}H_{17}NO_8$, $C_{15}H_{19}NO_8$, $C_{17}H_{27}NO_7$, and $C_8H_{11}NO_7$ and so on.

210   More than 77.7% of the CHON formulas in f_{RA} in all six samples have O/N ratios exceeding 3, indicating that the N atoms in

211   these molecules may be in the $-NO_3$ functional group (Zhao et al., 2013). Samples CL12-16 show no prominent peak of the

212   function classes in the N_2 category, but a dominant peak of the $-N_2O_5$ class is observed in CL17 (Fig. 4), where $C_8H_8N_2O_5$ and

213   $C_7H_6N_2O_5$ are two most abundant formulas. These formulas probably belong to dinitrophenols and their derivatives.

214   To evaluate the contribution of primary sources, we compared the molecular composition in cloud water with that in particles

215   emitted from the primary sources such as biomass burning (including corn straw, pine branches and rice straw) and coal

216   combustion using the same analytical instrument (Song et al., 2018). In cloud water, 40.9-51.4%, 21.9-27.1% and 48.1-59.4%

217   (in terms of number fraction) of CHON molecules appear in the smoke particles of corn straw, pine branches and rice straw,

218 indicating a non-negligible contribution from biomass burning. While only 10.5-14.5% of molecules in cloud water can be

219 corresponding to the coal combustion emission, suggesting the less contribution to the molecular composition of cloud water.

220 Note that the comparison only based on the molecular formulas given by FT-ICR MS, the isomeride cannot be distinguished,

221 thus the results only represents a possible relationship with the different sources. Additionally, some N-containing molecules

222 are also detected in monoterpene SOA (Park et al., 2017; Zhang et al., 2018), in which the products such as $C_7H_{9,11}NO_{7-8}$,

223 $C_8H_{11}NO_{7-8}$, $C_9H_{13,15}NO_{7-8}$, and $C_{10}H_{15,\mathbf{17},19}NO_{7-8}$ are detected in cloud water, indicating a contribution from monoterpene

224 oxidation.

225 **CHO** For CHO formulas in cloud water, a prominent C_{17} peak is observed in all six samples (Fig. S7), in which the most

226 abundant formula is $C_{17}H_{26}O_4$, which also causes a significant peak of O_4 class (Fig. 4). The formula may belong to lipids-like

227 compounds based on the classification in the VK plot (Bianco et al., 2018). Considering the intensive emission of biogenic

228 volatile organic compounds (BVOCs) around the sampling site, the oxidation products of BVOCs may also contribute to the

229 molecular composition. Putman et al. (2012) reported the molecular composition of α-pinene ozonolysis SOA using FT-ICR

230 MS. 26.9-39.1% (in term of number fraction) of the CHO formulas in cloud water are corresponding to the yields of α-pinene

231 ozonolysis, including the most abundant $C_{17}H_{26}O_4$, indicating possible contribution from BVOCs oxidation. In addition, cloud

232 water contains formulas that have been observed in the combustion of coal and biogenic materials. Specifically, 26.5-38.7%,

233 65.9-77.3%, 50.7-69.3%, and 61.1-76.7% of the CHO formulas in cloud water, by number, were detected in the smoke emitted

234 from combustion of coal, corn straw, pine branches, and rice straw, respectively (Song et al., 2018), indicating that combustion

235 also potentially contributes to the organics in cloud water.

236 **S-containing formulas** Most of the CHOS formulas in cloud water have C_{13} or C_{14} peaks (Fig. S7), and $-SO_3$ or $-SO_4$ represent

237 the most abundant classes of CHOS (Fig. 4). We divided the CHOS formulas into two classes according to the O/S ratios:

238 $CHOS_{O/S\geq4}$ and $CHOS_{O/S<4}$. When O/S ≥ 4, CHOS can be provisionally identified as organosulfates (Lin et al., 2012). The O/S

239 ratios of most of the CHOS formulas (78.9-95.8% in number fraction and 87.5-98.6% in f_{RA}) in cloud water exceed 4.

240 $CHOS_{O/S<4}$ accounts for 1.4-12.5% in f_{RA} of all the CHOS formulas in cloud water, indicating reduced S groups exist in these

241 formulas. Some of them are aliphatic-like, such as $C_{24}H_{42}O_3S$, $C_{29}H_{52}O_3S$. Some are aromatic-like with high DBE values, such

242 as $C_6H_6O_3S$, which may be an aromatic ring bearing a $–SO_3H$ group. Some of them may have more than one aromatic rings,

243 such as $C_{17}H_{16}O_3S$, $C_{20}H_{18}O_3S$. Note that the aromaticity of these formulas cannot be identified accurately using AI_{mod} values,

244 since the value is a conservative method to evaluate the aromaticity (Koch and Dittmar, 2006). The presence of aromatic

245 structure in these molecules indicates that they are likely emitted by anthropogenic sources or biomass burning (Ervens et al.,

246 2011). Most of the CHONS formulas clearly peak at C_{10} (Fig. S7) and have more than seven O atoms (Fig. 4), allowing the

247 presence of both sulfate and nitrate functional groups. These species can be nitrooxy organosulfates, which have been widely

248 observed in the cloud/fog water (Zhao et al., 2013; Brege et al., 2018) and aerosols (Wozniak et al., 2014). For the detected S-

249   containing formulas in cloud water, 6.2-23.0%, 15.9-33.6% and 15.0-34.3% in terms of number fraction are corresponding to

250   the molecules in particles emitted by burning of corn straw, pine branches, and rice straw, respectively, while 24.8-47.7%

251   (41.0% on arithmetic mean) are corresponding to that in coal combustion (Song et al., 2018), indicating coal combustion

252   contributes to S-containing formulas in cloud water more significantly compared with that to CHO and CHON.

253   **3.4 Organic matter formed by in-cloud aqueous-phase reactions**

254   **3.4.1 Formation of dinitrophenols**

255   To investigate the formation of molecules in cloud water, we compared the molecular formulas in cloud water with $PM_{2.5}$. For

256   CHON, the $-N_1O_8$ or $-N_1O_7$ formulas are also abundant in $PM_{2.5}$ samples (Fig. S5), suggesting that these formulas may not

257   only form in cloud water. However, the formulas with high intensities, e.g., $C_8H_8N_2O_5$, $C_7H_7N_2O_5$ and $C_6H_4N_2O_5$ in cloud

258   water are not detected in $PM_{2.5}$ samples. Earlier studies have found that over one-third of the nitrophenols and the majority of

259   the dinitrophenols are contributed by secondary formation (Harrison et al., 2005). The transforming from 2-nitrophenol into

260   2,4-dinitrophenol was also observed during cloud events (LüTtke et al., 1997; Lüttke et al., 1999). Aqueous-phase radical

261   nitration of mononitroaromatics has been reported to be a potential pathway to form dinitroaromatics (Lüttke et al., 1999;

262   Kroflic et al., 2015; Cook et al., 2017). This implies that in-cloud aqueous-phase reactions represent the main formation

263   pathway of dinitrophenols at the observation site.

264   Generally, CHON in cloud water has a higher f_{RA} during the nighttime (56.2-65.3%) compared with the daytime (43.6-54.9%)

265   (Table S5), which is consistent with the previous findings for aerosols (O'brien et al., 2014). Particularly, the RA of $-N_2O_5$

266   formulas increases significantly at night. The representative formulas including $C_6H_4N_2O_5$, $C_7H_6N_2O_5$, and $C_8H_8N_2O_5$ account

267   for 0.5%, 0.1%, 0.4%, 0.7%, 2.1%, and 14.8% of CHON in f_{RA} for samples CL12-17, respectively. This may attribute to the

268   aqueous-phase formation of these possible dinitrophenols at night. While during the daytime, the direct photolysis of

269   nitrophenols would release NO_2^- and NO_3^- (Harrison et al., 2005; Chen et al., 2005; Bejan et al., 2006), causing the observed

270   low RA of nitrophenols and dinitrophenols. Consistently, the five diurnal-nocturnal cycle samples (CL2-23) exhibit a higher

271   concentration of WSON at night compared with the daytime (Text S5, Fig. S3 and Table S2). A recent study conducted at the

272   Field Museum Tama Hill, Japan also observed that aerosol liquid water accelerated the formation of WSON, especially at

273   night, and the authors suggested that aqueous-phase reactions between NH_4^+/reactive nitrogen and BVOCs at night contribute

274   significantly to WSON in particles (Xu et al., 2020). While in this study, the elevated abundance of N-containing organics in

275   cloud water at night are mainly contributed by dinitrophenols and their derivatives, which are the products of radical nitration

276   in the aqueous phase, indicating a possible pathway for the generation of WSON.

277 **3.4.2 Formation of oxygenated organic matter and organosulfates**

278 For CHO, the most abundant $C_{17}H_{26}O_4$ in cloud water is not detected in the PM$_{2.5}$ samples, suggesting a formation by the in-

279 cloud aqueous-phase reactions, although the contribution from BVOCs cannot be ruled out. Interestingly, CHO formulas in

280 PM$_{2.5}$ samples peak at O$_8$ (Fig. S5), which is significantly higher than cloud water (Fig. 4). This is consistent with the higher

281 OS$_C$ values appear in PM$_{2.5}$ samples. Some highly oxidized molecules (HOMs, O/C ≥ 0.6), e.g., $C_7H_{10}O_5$, $C_8H_{12}O_5$, $C_{13}H_{24}O_{13}$,

282 are identified in cloud water, however, the HOMs in cloud water only account for 12.6-32.2% in terms of f_{RA}. A higher f_{RA} of

283 CHO is observed during the daytime (Fig. 1b), which may result from the photochemical oxidation (e.g., the oxidation of

284 volatile organic compounds, VOCs) (Ehn et al., 2014; Wang et al., 2017) and photolysis of N- and S-containing formulas in

285 cloud water under the illumination (Bruggemann et al., 2020; Laskin et al., 2015).

286 For CHOS formulas, the most abundant functions classes are similar between cloud water and PM$_{2.5}$, and no identifiable

287 difference of fraction of organosulfates is observed between cloud water and PM$_{2.5}$, which may indicate the multiphase

288 reactions and/or other common sources of CHOS in cloud water and PM$_{2.5}$. However, S-containing formulas are abundant at

289 night (8.4-20.9% in f_{RA}) compared with daytime (4.3-10.2% in f_{RA}).We note that the f_{RA} of CHOS$_{O/S≥4}$ at night (92.9-98.6%)

290 is slightly higher than that during the daytime (87.5-92.2%). Thus the formation of organosulfates likely enhances at night,

291 while the photochemical oxidation of organosulfates results in the release of inorganic sulfate during the daytime (Bruggemann

292 et al., 2020), causing a low fraction of organosulfates.

293 **4 Conclusions and Atmospheric Implications**

294 This study investigated the molecular characteristics of cloud water using FT-ICR MS. Thousands of formulas including CHO,

295 CHON, CHOS and CHONS were detected, in which CHON and CHO formulas are dominant. Although here we only include

296 one single diurnal cycle, and the contingency cannot be ruled out, this study highlights the important effects of in-cloud

297 aqueous-phase reactions on the molecular characteristics and composition of cloud water.

298 Previous studies expected a higher oxidation state of organics in cloud water, however, no statistically difference between

299 cloud water and PM$_{2.5}$ is observed in this study. While a higher OS$_C$ of detected formulas, especially CHO, appears in PM$_{2.5}$

300 samples. Most of formulas are identified as aliphatic and olefinic species, CHON and their aromatic structures are abundant

301 in cloud water. The complexity of aqueous-phase processes in the actual atmosphere appeal to the future researches.

302 Our results showed that N-containing formulas are the most abundant formulas in cloud water, which may relate to the

303 aqueous-phase formation. Dinitrophenols and derivatives exist abundantly in cloud water, especially at night, suggesting the

304 contribution on N-containing organics from radical nitration in cloud water. Meanwhile, organosulfates are also abundant in

305 cloud water, and a slightly higher fraction is observed at night, suggesting the dark-reaction formation. Nitroaromatic

306 compounds have been identified as one of the major light absorption components in brown carbon (Li et al., 2020b) and

307 regarded as the phytotoxin as well as suspected carcinogenic materials (Harrison et al., 2005). Organosulfates are thought to

308 affect the physicochemical properties of aerosol such as hygroscopicity and cloud condensation nuclei formation potential

309 (Bruggemann et al., 2020). Thus the aqueous-phase formation of N-containing organics and organosulfates at night are worth

310 targeting in the near future.

311

312

313 *Supplement.* Supporting information includes five texts (Text S1-S5), seven figures (Fig. S1-S7) and seven tables (Table S1-

314 S7) related to the manuscript.

315

316 *Data availability.* The raw data of this study can be obtained by contacting the corresponding author.

317

318 *Author contributions.* XB and GZ design the research with input from XW, PP and GS. YF, FJ and YY collected samples. WS,

319 BJ carried out the sample pretreatment and instrumental analysis under the guidance of YL. WS processed data when YF and

320 XL gave constructive discussion. WS wrote the manuscript, and XB, GZ and YF interpreted data and edited the manuscript.

321 JC, DC, and JO had an active role in supporting the sampling work. All authors contributed to the discussions of the results

322 and refinement of the manuscript.

323

324 *Competing interests.* The authors declare that they have no conflict of interest.

325

326 *Acknowledgements.* The authors gratefully acknowledge Jianzhong Song and Chunlin Zou (Guangzhou Institute of

327 Geochemistry, Chinese Academy of Sciences) for the guidance and assistance during sample pretreatment and providing the

328 raw data related to the article *Song et al., 2018*, which is helpful to the discussion of this manuscript.

329

330 *Financial support.* This work was supported by National Nature Science Foundation of China (41877307 and 42077322),

331 Natural Science Foundation of Guangdong Province (2019B151502022), and Guangdong Foundation for Program of Science

332 and Technology Research (2019B121202002 and 2019B121205006).

333

334 **References**

335 An, Y., Xu, J., Feng, L., Zhang, X., Liu, Y., Kang, S., Jiang, B., and Liao, Y.: Molecular characterization of organic aerosol

336   in the Himalayas: insight from ultra-high-resolution mass spectrometry, Atmos. Chem. Phys., 19, 1115-1128,

337   https://doi.org/10.5194/acp-19-1115-2019, 2019.

338 Bejan, I., Abd El Aal, Y., Barnes, I., Benter, T., Bohn, B., Wiesen, P., and Kleffmann, J.: The photolysis of ortho-nitrophenols:

339   a new gas phase source of HONO, Phys. Chem. Chem. Phys., 8, 2028-2035, https://doi.org/10.1039/B516590C, 2006.

340 Bianco, A., Passananti, M., Deguillaume, L., Mailhot, G., and Brigante, M.: Tryptophan and tryptophan-like substances in

341   cloud   water: Occurrence   and   photochemical   fate,   Atmos.   Environ.,   137,   53-61,

342   https://doi.org/10.1016/j.atmosenv.2016.04.034, 2016a.

343 Bianco, A., Voyard, G., Deguillaume, L., Mailhot, G., and Brigante, M.: Improving the characterization of dissolved organic

344   carbon in cloud water: Amino acids and their impact on the oxidant capacity, Sci. Rep., 6, 37420,

345   https://doi.org/10.1038/srep37420, 2016b.

346 Bianco, A., Deguillaume, L., Vaitilingom, M., Nicol, E., Baray, J. L., Chaumerliac, N., and Bridoux, M.: Molecular

347   Characterization of Cloud Water Samples Collected at the Puy de Dome (France) by Fourier Transform Ion Cyclotron

348   Resonance Mass Spectrometry, Environ. Sci. Technol., 52, 10275-10285, https://doi.org/10.1021/acs.est.8b01964, 2018.

349 Bianco, A., Riva, M., Baray, J.-L., Ribeiro, M., Chaumerliac, N., George, C., Bridoux, M., and Deguillaume, L.: Chemical

350   Characterization of Cloudwater Collected at Puy de Dôme by FT-ICR MS Reveals the Presence of SOA Components,

351   ACS Earth Space Chem., 3, 2076-2087, https://doi.org/10.1021/acsearthspacechem.9b00153, 2019.

352 Blando, J. D. and Turpin, B. J.: Secondary organic aerosol formation in cloud and fog droplets: a literature evaluation of

353   plausibility, Atmos. Environ., 34, 1623-1632, https://doi.org/10.1016/S1352-2310(99)00392-1, 2000.

354 Boone, E. J., Laskin, A., Laskin, J., Wirth, C., Shepson, P. B., Stirm, B. H., and Pratt, K. A.: Aqueous Processing of

355   Atmospheric Organic Particles in Cloud Water Collected via Aircraft Sampling, Environ. Sci. Technol., 49, 8523-8530,

356   https://doi.org/10.1021/acs.est.5b01639, 2015.

357 Braman, T., Dolvin, L., Thrasher, C., Yu, H., Walhout, E. Q., and O'Brien, R. E.: Fresh versus Photo-recalcitrant Secondary

358   Organic Aerosol: Effects of Organic Mixtures on Aqueous Photodegradation of 4-Nitrophenol, Environ. Sci. Technol.

359   Lett., 7, 248-253, https://doi.org/10.1021/acs.estlett.0c00177, 2020.

360 Brege, M., Paglione, M., Gilardoni, S., Decesari, S., Facchini, M. C., and Mazzoleni, L. R.: Molecular insights on aging and

361   aqueous-phase processing from ambient biomass burning emissions-influenced Po Valley fog and aerosol, Atmos. Chem.

362   Phys., 18, 13197-13214, https://doi.org/10.5194/acp-18-13197-2018, 2018.

363   Bruggemann, M., Xu, R., Tilgner, A., Kwong, K. C., Mutzel, A., Poon, H. Y., Otto, T., Schaefer, T., Poulain, L., Chan, M. N.,
364   and Herrmann, H.: Organosulfates in Ambient Aerosol: State of Knowledge and Future Research Directions on Formation,
365   Abundance, Fate, and Importance, Environ. Sci. Technol., 54, 3767-3782, https://doi.org/10.1021/acs.est.9b06751, 2020.

366   Chen, B., Yang, C., and Goh, N. K.: Direct photolysis of nitroaromatic compounds in aqueous solutions, J. Environ. Sci. China,
367   17, 598-604, https://doi.org/10.1016/S1001-0742(06)60039-9, 2005.

368   Cho, Y., Ahmed, A., Islam, A., and Kim, S.: Developments in FT-ICR MS instrumentation, ionization techniques, and data
369   interpretation methods for petroleomics, Mass. Spectrom. Rev., 34, 248-263, https://doi.org/10.1002/mas.21438, 2015.

370   Cook, R., Lin, Y.-H., Peng, Z., Boone, E., Chu, R. K., Dukett, J. E., Gunsch, M. J., Zhang, W., Tolic, N., Laskin, A., and Pratt,
371   K. A.: Biogenic, urban, and wildfire influences on the molecular composition of dissolved organic compounds in cloud
372   water, Atmos. Chem. Phys., 17, 15167-15180, https://doi.org/10.5194/acp-17-15167-2017, 2017.

373   De Haan, D. O., Hawkins, L. N., Kononenko, J. A., Turley, J. J., Corrigan, A. L., Tolbert, M. A., and Jimenez, J. L.: Formation
374   of nitrogen-containing oligomers by methylglyoxal and amines in simulated evaporating cloud droplets, Environ. Sci.
375   Technol., 45, 984-991, https://doi.org/10.1021/es102933x, 2011.

376   De Haan, D. O., Corrigan, A. L., Smith, K. W., Stroik, D. R., Turley, J. J., Lee, F. E., Tolbert, M. A., Jimenez, J. L., Cordova,
377   K. E., and Ferrell, G. R.: Secondary Organic Aerosol-Forming Reactions of Glyoxal with Amino Acids, Environ. Sci.
378   Technol., 43, 2818-2824, https://doi.org/10.1021/es803534f, 2009.

379   De Haan, D. O., Tapavicza, E., Riva, M., Cui, T., Surratt, J. D., Smith, A. C., Jordan, M. C., Nilakantan, S., Almodovar, M.,
380   Stewart, T. N., de Loera, A., De Haan, A. C., Cazaunau, M., Gratien, A., Pangui, E., and Doussin, J. F.: Nitrogen-
381   Containing, Light-Absorbing Oligomers Produced in Aerosol Particles Exposed to Methylglyoxal, Photolysis, and Cloud
382   Cycling, Environ. Sci. Technol., 52, 4061-4071, https://doi.org/10.1021/acs.est.7b06105, 2018.

383   Deguillaume, L., Leriche, M., Desboeufs, K., Mailhot, G., George, C., and Chaumerliac, N.: Transition Metals in Atmospheric
384   Liquid Phases: Sources, Reactivity, and Sensitive Parameters, Chem. Rev., 105, 3388-3431,
385   https://doi.org/10.1021/cr040649c, 2005.

386   Demoz, B. B., Collett Jr, J. L., and Daube Jr, B. C.: On the Caltech Active Strand Cloudwater Collectors, Atmos. Res., 41, 47-
387   62, https://doi.org/10.1016/0169-8095(95)00044-5, 1996.

388   Ehn, M., Thornton, J. A., Kleist, E., Sipila, M., Junninen, H., Pullinen, I., Springer, M., Rubach, F., Tillmann, R., Lee, B.,
389   Lopez-Hilfiker, F., Andres, S., Acir, I. H., Rissanen, M., Jokinen, T., Schobesberger, S., Kangasluoma, J., Kontkanen, J.,
390   Nieminen, T., Kurten, T., Nielsen, L. B., Jorgensen, S., Kjaergaard, H. G., Canagaratna, M., Maso, M. D., Berndt, T.,
391   Petaja, T., Wahner, A., Kerminen, V. M., Kulmala, M., Worsnop, D. R., Wildt, J., and Mentel, T. F.: A large source of
392   low-volatility secondary organic aerosol, Nature, 506, 476-479, https://doi.org/10.1038/nature13032, 2014.

393   Ehrenhauser, F. S., Khadapkar, K., Wang, Y., Hutchings, J. W., Delhomme, O., Kommalapati, R. R., Herckes, P., Wornat, M.

394   J., and Valsaraj, K. T.: Processing of atmospheric polycyclic aromatic hydrocarbons by fog in an urban environment, J.

395   Environ. Monitor., 14, 2566-2579, https://doi.org/10.1039/c2em30336a, 2012.

396   Ervens, B., Turpin, B. J., and Weber, R. J.: Secondary organic aerosol formation in cloud droplets and aqueous particles

397   (aqSOA): a review of laboratory, field and model studies, Atmos. Chem. Phys., 11, 11069-11102,

398   https://doi.org/10.5194/acp-11-11069-2011, 2011.

399   Ervens, B., Wang, Y., Eagar, J., Leaitch, W. R., Macdonald, A. M., Valsaraj, K. T., and Herckes, P.: Dissolved organic carbon

400   (DOC) and select aldehydes in cloud and fog water: the role of the aqueous phase in impacting trace gas budgets, Atmos.

401   Chem. Phys., 13, 5117-5135, https://doi.org/10.5194/acp-13-5117-2013, 2013.

402   Ge, X., Zhang, Q., Sun, Y., Ruehl, C. R., and Setyan, A.: Effect of aqueous-phase processing on aerosol chemistry and size

403   distributions in Fresno, California, during wintertime, Environ. Chem., 9, 221-235, https://doi.org/10.1071/en11168, 2012.

404   Hallquist, M., Wenger, J. C., Baltensperger, U., Rudich, Y., Simpson, D., Claeys, M., Dommen, J., Donahue, N. M., George,

405   C., Goldstein, A. H., Hamilton, J. F., Herrmann, H., Hoffmann, T., Linuma, Y., Jang, M., Jenkin, M. E., Jimenez, J. L.,

406   Kiendler-Scharr, A., Maenhaut, W., McFiggans, G., Mentel, T. F., Monod, A., Prévôt, A. S. H., Seinfeld, J. H., Surratt,

407   J. D., Szmigielski, R., and Wildt, J.: The formation, properties and impact of secondary organic aerosol: Current and

408   emerging issues, Atmos. Chem. Phys., 9, 5155–5236, https://doi.org/10.5194/acp-9-5155-2009, 2009.

409   Harrison, M. A. J., Barra, S., Borghesi, D., Vione, D., Arsene, C., and Iulian Olariu, R.: Nitrated phenols in the atmosphere: a

410   review, Atmos. Environ., 39, 231-248, https://doi.org/10.1016/j.atmosenv.2004.09.044, 2005.

411   Herckes, P., Valsaraj, K. T., and Collett, J. L.: A review of observations of organic matter in fogs and clouds: Origin, processing

412   and fate, Atmos. Res., 132-133, 434-449, https://doi.org/10.1016/j.atmosres.2013.06.005, 2013.

413   Herckes, P., Hannigan, M. P., Trenary, L., Lee, T., and Collett Jr, J. L.: Organic compounds in radiation fogs in Davis

414   (California), Atmos. Res., 64, 99-108, https://doi.org/10.1016/S0169-8095(02)00083-2, 2002.

415   Herrmann, H., Hoffmann, D., Schaefer, T., Brauer, P., and Tilgner, A.: Tropospheric aqueous-phase free-radical chemistry:

416   radical   sources,   spectra,   reaction   kinetics   and   prediction   tools,   Chemphyschem,   11,   3796-3822,

417   https://doi.org/10.1002/cphc.201000533, 2010.

418   Herrmann, H., Schaefer, T., Tilgner, A., Styler, S. A., Weller, C., Teich, M., and Otto, T.: Tropospheric aqueous-phase

419   chemistry: kinetics, mechanisms, and its coupling to a changing gas phase, Chem. Rev., 115, 4259-4334,

420   https://doi.org/10.1021/cr500447k, 2015.

421   Hockaday, W. C., Grannas, A. M., Kim, S., and Hatcher, P. G.: Direct molecular evidence for the degradation and mobility of

422   black carbon in soils from the ultrahigh-resolution mass spectral analysis of dissolved organic matter from a fire-impacted

423   forest soil, Org. Geochem., 37, 501-510, https://doi.org/10.1016/j.orggeochem.2005.11.003, 2006.

424 Huang, D. D., Zhang, Q., Cheung, H. H. Y., Yu, L., Zhou, S., Anastasio, C., Smith, J. D., and Chan, C. K.: Formation and
425   Evolution of aqSOA from Aqueous-Phase Reactions of Phenolic Carbonyls: Comparison between Ammonium Sulfate
426   and Ammonium Nitrate Solutions, Environ. Sci. Technol., 52, 9215-9224, https://doi.org/10.1021/acs.est.8b03441, 2018.

427 Kim, H., Collier, S., Ge, X., Xu, J., Sun, Y., Jiang, W., Wang, Y., Herckes, P., and Zhang, Q.: Chemical processing of water-
428   soluble species and formation of secondary organic aerosol in fogs, Atmos. Environ., 200, 158-166,
429   https://doi.org/10.1016/j.atmosenv.2018.11.062, 2019.

430 Koch, B. P. and Dittmar, T.: From mass to structure: an aromaticity index for high-resolution mass data of natural organic
431   matter, Rapid Commun. Mass Sp., 20, 926-932, https://doi.org/10.1002/rcm.2386, 2006.

432 Kroflic, A., Grilc, M., and Grgic, I.: Does toxicity of aromatic pollutants increase under remote atmospheric conditions?, Sci.
433   Rep., 5, 8859, https://doi.org/10.1038/srep08859, 2015.

434 Kroll, J. H., Donahue, N. M., Jimenez, J. L., Kessler, S. H., Canagaratna, M. R., Wilson, K. R., Altieri, K. E., Mazzoleni, L.
435   R., Wozniak, A. S., Bluhm, H., Mysak, E. R., Smith, J. D., Kolb, C. E., and Worsnop, D. R.: Carbon oxidation state as a
436   metric   for   describing   the   chemistry   of   atmospheric   organic   aerosol,   Nat.   Chem.,   3,   133-139,
437   https://doi.org/10.1038/nchem.948, 2011.

438 Kua, J., Krizner, H. E., and De Haan, D. O.: Thermodynamics and kinetics of imidazole formation from glyoxal, methylamine,
439   and formaldehyde: a computational study, J. Phys. Chem. A, 115, 1667-1675, https://doi.org/10.1021/jp111527x, 2011.

440 L.oflund, M., Kasper-Giebl, A., Schuster, B., Giebl, H., Hitzenberger, R., and Puxbaum, H.: Formic, acetic, oxalic, malonic
441   andsuccinic acid concentrations andtheir contribution to organic carbon in cloudwater, Atmos. Environ., 36, 1553–1558,
442   https://doi.org/10.1016/S1352-2310(01)00573-8, 2002.

443 Laskin, A., Laskin, J., and Nizkorodov, S. A.: Chemistry of atmospheric brown carbon, Chem. Rev., 115, 4335-4382,
444   https://doi.org/10.1021/cr5006167, 2015.

445 Leclair, J. P., Collett, J. L., and Mazzoleni, L. R.: Fragmentation analysis of water-soluble atmospheric organic matter using
446   ultrahigh-resolution   FT-ICR   mass   spectrometry,   Environ.   Sci.   Technol.,   46,   4312-4322,
447   https://doi.org/10.1021/es203509b, 2012.

448 Li, T., Wang, Z., Wang, Y., Wu, C., Liang, Y., Xia, M., Yu, C., Yun, H., Wang, W., Wang, Y., Guo, J., Herrmann, H., and
449   Wang, T.: Chemical characteristics of cloud water and the impacts on aerosol properties at a subtropical mountain site in
450   Hong Kong SAR, Atmos. Chem. Phys., 20, 391–407, https://doi.org/10.5194/acp-2019-481, 2020a.

451 Li, X., Wang, Y., Hu, M., Tan, T., Li, M., Wu, Z., Chen, S., and Tang, X.: Characterizing chemical composition and light
452   absorption   of   nitroaromatic   compounds   in   the   winter   of   Beijing,   Atmos.   Environ.,   237,   117712,
453   https://doi.org/10.1016/j.atmosenv.2020.117712, 2020b.

454   Li, Y. J., Huang, D. D., Cheung, H. Y., Lee, A. K. Y., and Chan, C. K.: Aqueous-phase photochemical oxidation and direct

455   photolysis of vanillin – a model compound of methoxy phenols from biomass burning, Atmos. Chem. Phys., 14, 2871-

456   2885, https://doi.org/10.5194/acp-14-2871-2014, 2014.

457   Lin, P., Yu, J. Z., Engling, G., and Kalberer, M.: Organosulfates in humic-like substance fraction isolated from aerosols at

458   seven locations in East Asia: a study by ultra-high-resolution mass spectrometry, Environ. Sci. Technol., 46, 13118-13127,

459   https://doi.org/10.1021/es303570v, 2012.

460   Lin, Q., Zhang, G., Peng, L., Bi, X., Wang, X., Brechtel, F. J., Li, M., Chen, D., Peng, P., amp, apos, an, Sheng, G., and Zhou,

461   Z.: In situ chemical composition measurement of individual cloud residue particles at a mountain site, southern China,

462   Atmos. Chem. Phys., 17, 8473-8488, https://doi.org/10.5194/acp-17-8473-2017, 2017.

463   Lüttke, J., Levsen, K., Acker, K., Wieprecht, W., and Möller, D.: Phenols and Nitrated Phenols in Clouds at Mount Brocken,

464   Int. J. Environ. An. Ch., 74, 69-89, https://doi.org/10.1080/03067319908031417, 1999.

465   Lüttke, J., Scheer, V., Levsen, K., Wu¨nsch, G., Cape, J. N., Hargreaves, K. J., Storeton-West, R. L., Acker, K., Wieprecht,

466   W., and Jones, B.: Occurrence and formation of nitrated phenols in and out of cloud, Atmos. Environ., 2637–2648,

467   https://doi.org/10.1016/S1352-2310(96)00229-4, 1997.

468   Mazzoleni, L. R., Saranjampour, P., Dalbec, M. M., Samburova, V., Hallar, A. G., Zielinska, B., Lowenthal, D. H., and Kohl,

469   S.: Identification of water-soluble organic carbon in non-urban aerosols using ultrahigh-resolution FT-ICR mass

470   spectrometry: organic anions, Environ. Chem., 9, 285, https://doi.org/10.1071/en11167, 2012.

471   McNeill, V. F.: Aqueous organic chemistry in the atmosphere: sources and chemical processing of organic aerosols, Environ.

472   Sci. Technol., 49, 1237-1244, https://doi.org/10.1021/es5043707, 2015.

473   O'Brien, R. E., Laskin, A., Laskin, J., Rubitschun, C. L., Surratt, J. D., and Goldstein, A. H.: Molecular characterization of S-

474   and N-containing organic constituents in ambient aerosols by negative ion mode high-resolution Nanospray Desorption

475   Electrospray Ionization Mass Spectrometry: CalNex 2010 field study, J. Geophys. Res.: Atmos., 119, 12,706-712,720,

476   https://doi.org/10.1002/2014jd021955, 2014.

477   Paglione, M., Gilardoni, S., Rinaldi, M., Decesari, S., Zanca, N., Sandrini, S., Giulianelli, L., Bacco, D., Ferrari, S., Poluzzi,

478   V., Scotto, F., Trentini, A., Poulain, L., Herrmann, H., Wiedensohler, A., Canonaco, F., Prévôt, A. S. H., Massoli, P.,

479   Carbone, C., Facchini, M. C., and Fuzzi, S.: The impact of biomass burning and aqueous-phase processing on air quality:

480   a multi-year source apportionment study in the Po Valley, Italy, Atmos. Chem. Phys., 20, 1233–1254,

481   https://doi.org/10.5194/acp-2019-274, 2020.

482   Park, J.-H., Babar, Z. B., Baek, S. J., Kim, H. S., and Lim, H.-J.: Effects of NO x on the molecular composition of secondary

483   organic aerosol formed by the ozonolysis and photooxidation of α-pinene, Atmos. Environ., 166, 263-275,

484   https://doi.org/10.1016/j.atmosenv.2017.07.022, 2017.

485   Putman, A. L., Offenberg, J. H., Fisseha, R., Kundu, S., Rahn, T. A., and Mazzoleni, L. R.: Ultrahigh-resolution FT-ICR mass
486   spectrometry characterization of α-pinene ozonolysis SOA, Atmos. Environ., 46, 164-172,
487   https://doi.org/10.1016/j.atmosenv.2011.10.003, 2012.

488   Reed Harris, A. E., Ervens, B., Shoemaker, R. K., Kroll, J. A., Rapf, R. J., Griffith, E. C., Monod, A., and Vaida, V.:
489   Photochemical kinetics of pyruvic acid in aqueous solution, J. Phys. Chem. A, 118, 8505-8516,
490   https://doi.org/10.1021/jp502186q, 2014.

491   Renard, P., Siekmann, F., Salque, G., Demelas, C., Coulomb, B., Vassalo, L., Ravier, S., Temime-Roussel, B., Voisin, D., and
492   Monod, A.: Aqueous-phase oligomerization of methyl vinyl ketone through photooxidation - Part 1: Aging processes of
493   oligomers, Atmos. Chem. Phys., 15, 21-35, https://doi.org/10.5194/acp-15-21-2015, 2015.

494   Rudziński, K. J. and Szmigielski, R.: Aqueous Reactions of Sulfate Radical-Anions with Nitrophenols in Atmospheric Context,
495   Atmosphere, 10, 795-809, https://doi.org/10.3390/atmos10120795, 2019.

496   Sareen, N., Carlton, A. G., Surratt, J. D., Gold, A., Lee, B., Lopez-Hilfiker, F. D., Mohr, C., Thornton, J. A., Zhang, Z., Lim,
497   Y. B., and Turpin, B. J.: Identifying precursors and aqueous organic aerosol formation pathways during the SOAS
498   campaign, Atmos. Chem. Phys., 16, 14409-14420, https://doi.org/10.5194/acp-16-14409-2016, 2016.

499   Schurman, M. I., Boris, A., Desyaterik, Y., and Collett, J. L.: Aqueous Secondary Organic Aerosol Formation in Ambient
500   Cloud Water Photo-Oxidations, Aerosol Air Qual. Res., 18, 15-25, https://doi.org/10.4209/aaqr.2017.01.0029, 2018.

501   Shi, Q., Pan, N., Long, H., Cui, D., Guo, X., Long, Y., Chung, K. H., Zhao, S., Xu, C., and Hsu, C. S.: Characterization of
502   Middle-Temperature Gasification Coal Tar. Part 3: Molecular Composition of Acidic Compounds, Energ. Fuel., 27, 108-
503   117, https://doi.org/10.1021/ef301431y, 2012.

504   Sleighter, R. L., Liu, Z., Xue, J., and Hatcher, P. G.: Multivariate Statistical Approaches for the Characterization of Dissolved
505   Organic Matter Analyzed by Ultrahigh Resolution Mass Spectrometry, Environ. Sci. Technol., 44, 7576–7582,
506   https://doi.org/10.1021/es1002204, 2010.

507   Smith, J. D., Sio, V., Yu, L., Zhang, Q., and Anastasio, C.: Secondary organic aerosol production from aqueous reactions of
508   atmospheric phenols with an organic triplet excited state, Environ. Sci. Technol., 48, 1049-1057,
509   https://doi.org/10.1021/es4045715, 2014.

510   Song, J., Li, M., Jiang, B., Wei, S., Fan, X., and Peng, P.: Molecular Characterization of Water-Soluble Humic like Substances
511   in Smoke Particles Emitted from Combustion of Biomass Materials and Coal Using Ultrahigh-Resolution Electrospray
512   Ionization Fourier Transform Ion Cyclotron Resonance Mass Spectrometry, Environ. Sci. Technol., 52, 2575-2585,
513   https://doi.org/10.1021/acs.est.7b06126, 2018.

514   Stein, A. F., Draxler, R. R., Rolph, G. D., Stunder, B. J. B., Cohen, M. D., and Ngan, F.: NOAA's HYSPLIT Atmospheric
515   Transport and Dispersion Modeling System, B. Am. Meteorol. Soc., 96, 2059-2077, https://doi.org/10.1175/bams-d-14-

516   00110.1, 2015.

517   Stubenrauch, C. J., Rossow, W. B., Kinne, S., Ackerman, S., Cesana, G., Chepfer, H., Di Girolamo, L., Getzewich, B.,

518   Guignard, A., Heidinger, A., Maddux, B. C., Menzel, W. P., Minnis, P., Pearl, C., Platnick, S., Poulsen, C., Riedi, J., Sun-

519   Mack, S., Walther, A., Winker, D., Zeng, S., and Zhao, G.: Assessment of Global Cloud Datasets from Satellites: Project

520   and Database Initiated by the GEWEX Radiation Panel, B. Am. Meteorol. Soc., 94, 1031-1049,

521   https://doi.org/10.1175/bams-d-12-00117.1, 2013.

522   Sun, X., Wang, Y., Li, H., Yang, X., Sun, L., Wang, X., Wang, T., and Wang, W.: Organic acids in cloud water and rainwater

523   at a mountain site in acid rain areas of South China, Environ. Sci. Pollut. Res. Int., 23, 9529-9539,

524   https://doi.org/10.1007/s11356-016-6038-1, 2016.

525   Sun, Y. L., Zhang, Q., Anastasio, C., and Sun, J.: Insights into secondary organic aerosol formed via aqueous-phase reactions

526   of phenolic compounds based on high resolution mass spectrometry, Atmos. Chem. Phys., 10, 4809-4822,

527   https://doi.org/10.5194/acp-10-4809-2010, 2010.

528   Szmigielski, R.: Evidence for C5 organosulfur secondary organic aerosol components from in-cloud processing of isoprene:

529   Role of reactive SO4 and SO3 radicals, Atmos. Environ., 130, 14-22, https://doi.org/10.1016/j.atmosenv.2015.10.072,

530   2016.

531   van Pinxteren, D., Fomba, K. W., Mertes, S., Müller, K., Spindler, G., Schneider, J., Lee, T., Collett, J. L., and Herrmann, H.:

532   Cloud water composition during HCCT-2010: Scavenging efficiencies, solute concentrations, and droplet size

533   dependence of inorganic ions and dissolved organic carbon, Atmos. Chem. Phys., 16, 3185-3205,

534   https://doi.org/10.5194/acp-16-3185-2016, 2016.

535   Wang, D., Li, Y., Yang, M., and Han, M.: Decomposition of polycyclic aromatic hydrocarbons in atmospheric aqueous

536   droplets through sulfate anion radicals: an experimental and theoretical study, Sci. Total. Environ., 393, 64-71,

537   https://doi.org/10.1016/j.scitotenv.2007.11.036, 2008.

538   Wang, M., Perroux, H., Fleuret, J., Bianco, A., Bouvier, L., Colomb, A., Borbon, A., and Deguillaume, L.: Anthropogenic and

539   biogenic hydrophobic VOCs detected in clouds at the puy de Dôme station using Stir Bar Sorptive Extraction: Deviation

540   from the Henry's law prediction, Atmos. Res., 237, https://doi.org/10.1016/j.atmosres.2020.104844, 2020.

541   Wang, S., Wu, R., Berndt, T., Ehn, M., and Wang, L.: Formation of Highly Oxidized Radicals and Multifunctional Products

542   from the Atmospheric Oxidation of Alkylbenzenes, Environ. Sci. Technol., 51, 8442-8449,

543   https://doi.org/10.1021/acs.est.7b02374, 2017.

544   Wozniak, A. S., Willoughby, A. S., Gurganus, S. C., and Hatcher, P. G.: Distinguishing molecular characteristics of aerosol

545   water soluble organic matter from the 2011 trans-North Atlantic US GEOTRACES cruise, Atmos. Chem. Phys., 14, 8419-

546   8434, https://doi.org/10.5194/acp-14-8419-2014, 2014.

547   Xu, Y., Miyazaki, Y., Tachibana, E., Sato, K., Ramasamy, S., Mochizuki, T., Sadanaga, Y., Nakashima, Y., Sakamoto, Y.,

548   Matsuda, K., and Kajii, Y.: Aerosol Liquid Water Promotes the Formation of Water-Soluble Organic Nitrogen in

549   Submicrometer Aerosols in a Suburban Forest, Environ. Sci. Technol., 54, 1406-1414,

550   https://doi.org/10.1021/acs.est.9b05849, 2020.

551   Yu, L., Smith, J., Laskin, A., George, K. M., Anastasio, C., Laskin, J., Dillner, A. M., and Zhang, Q.: Molecular transformations

552   of phenolic SOA during photochemical aging in the aqueous phase: competition among oligomerization, functionalization,

553   and fragmentation, Atmos. Chem. Phys., 16, 4511-4527, https://doi.org/10.5194/acp-16-4511-2016, 2016.

554   Zhang, H., Yee, L. D., Lee, B. H., Curtis, M. P., Worton, D. R., Isaacman-VanWertz, G., Offenberg, J. H., Lewandowski, M.,

555   Kleindienst, T. E., Beaver, M. R., Holder, A. L., Lonneman, W. A., Docherty, K. S., Jaoui, M., Pye, H. O. T., Hu, W.,

556   Day, D. A., Campuzano-Jost, P., Jimenez, J. L., Guo, H., Weber, R. J., de Gouw, J., Koss, A. R., Edgerton, E. S., Brune,

557   W., Mohr, C., Lopez-Hilfiker, F. D., Lutz, A., Kreisberg, N. M., Spielman, S. R., Hering, S. V., Wilson, K. R., Thornton,

558   J. A., and Goldstein, A. H.: Monoterpenes are the largest source of summertime organic aerosol in the southeastern United

559   States, P. Nat. Acad. Sci. USA, 115, 2038-2043, https://doi.org/10.1073/pnas.1717513115, 2018.

560   Zhao, Y., Hallar, A. G., and Mazzoleni, L. R.: Atmospheric organic matter in clouds: exact masses and molecular formula

561   identification using ultrahigh-resolution FT-ICR mass spectrometry, Atmos. Chem. Phys., 13, 12343-12362,

562   https://doi.org/10.5194/acp-13-12343-2013, 2013.

563

564
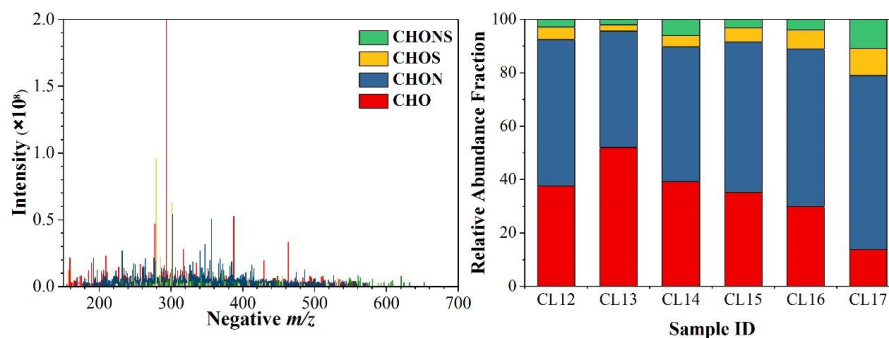
Figure 1. Reconstructed FT-ICR mass spectra of a typical sample, CL12 (a); Relative abundance fraction of the four groups (CHO, CHON, CHOS, and CHONS) in the six cloud water samples (b).

569

570
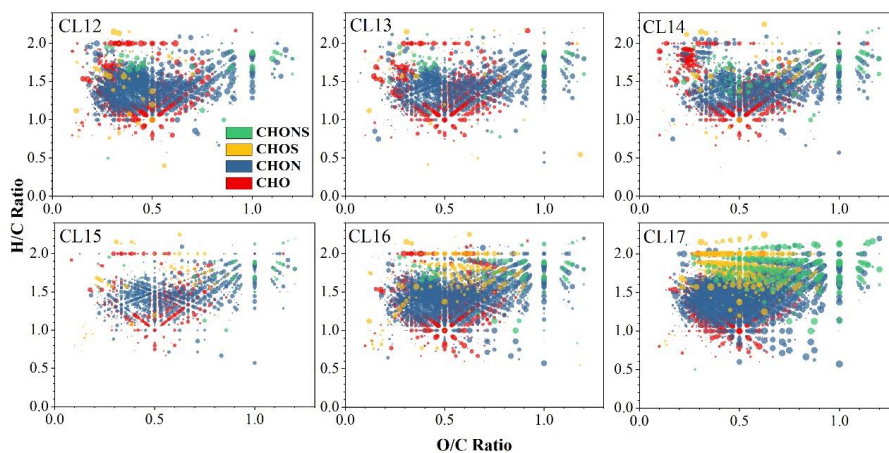
Figure 2. Van Krevelen diagrams as a function of four groups (CHO, CHNO, CHOS, and CHNOS) for the cloud water samples.

The larger point in the diagram represents the higher relative abundance of the formula.

573

574
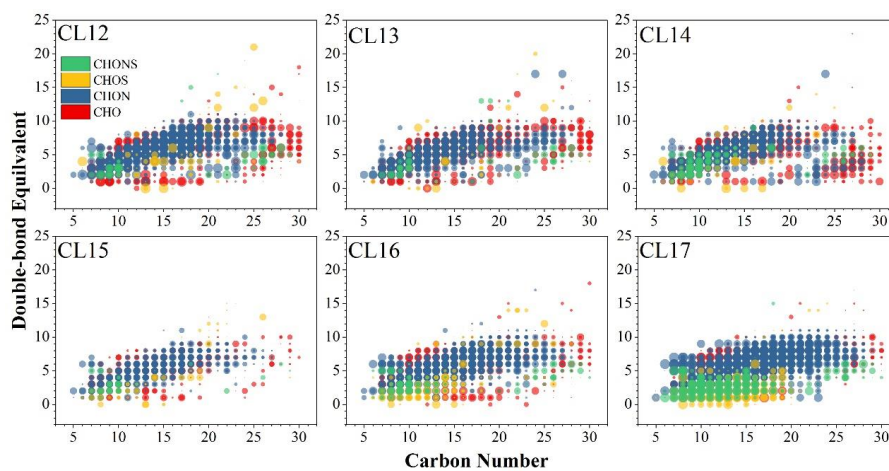
Figure 3. The double bond equivalent (DBE) versus the number of C atoms for unique molecular formulas in cloud water samples.

575

The larger point in the diagram represents the higher relative abundance of the compound.

576

577

578
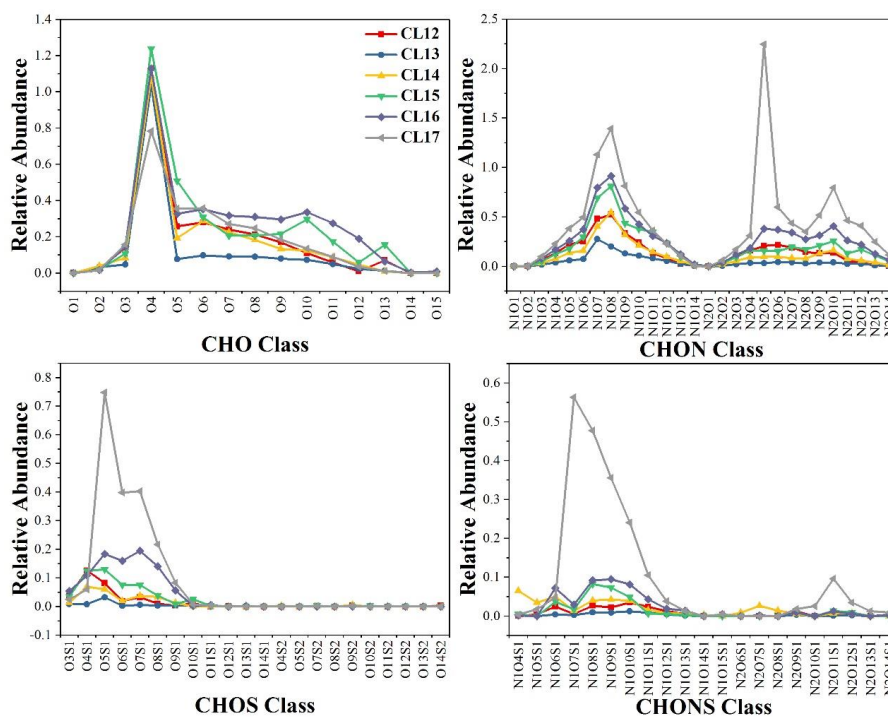
579

580 **Figure 4.** Relative abundance of the categories of CHO, CHON, CHOS and CHONS compounds according to the characteristic atom

581 **groups in the molecular formulas in cloud water.**

582

585

Table 1. The sampling interval, liquid water content (LWC, g m^{-3}), and pH of each sample. The calculation of LWC and the measurement of the pH values were described in Text S1 in Supporting Information.

Time	Sample ID	Sampling Interval	LWC	pH
Daytime	CL12	2018/5/11 10:15-12:40	0.17	4.16
	CL13	2018/5/11 12:40-15:00	0.17	4.22
	CL14	2018/5/11 15:00-18:00	0.19	4.37
Nighttime	CL15	2018/5/11 18:00-21:00	0.17	4.28
	CL16	2018/5/11 21:00-24:00	0.16	4.18
	CL17	2018/5/12 00:00-08:15	0.12	4.13

588

589